Reduced-order Structure-preserving Model for Parallel-connected Three-phase Grid-tied Inverters

Victor Purba, Sairaj V. Dhople
Department of ECE
University of Minnesota
E-mails: {purba002,sdhople}@umn.edu

Saber Jafarpour, Francesco Bullo
Department of Mechanical Engineering
University of California at Santa Barbara
E-mails: {saber.jafarpour,bullo}@engineering.ucsb.edu

Brian B. Johnson
National Renewable Energy Laboratory
Golden, Colorado
E-mail: brian.johnson@nrel.gov

***Abstract*—Next-generation power networks will contain large numbers of grid-connected inverters satisfying a significant fraction of system load. Since each inverter model has a relatively large number of dynamic states, it is impractical to analyze complex system models where the full dynamics of each inverter are retained. To address this challenge, we derive a reduced-order structure-preserving model for parallel-connected grid-tied three-phase inverters. Here, each inverter in the system is assumed to have a full-bridge topology, LCL filter at the point of common coupling, and the control architecture for each inverter includes a current controller, a power controller, and a phase-locked loop for grid synchronization. We outline a structure-preserving reduced-order inverter model with lumped parameters for the setting where the parallel inverters are each designed such that the filter components and controller gains scale linearly with the power rating. By structure preserving, we mean that the reduced-order three-phase inverter model is also composed of an LCL filter, a power controller, current controller, and PLL. We show that the system of parallel inverters can be modeled exactly as one aggregated inverter unit and this equivalent model has the same number of dynamical states as any individual inverter in the system. Numerical simulations validate the reduced-order model.**

I. Introduction

Distribution networks are witnessing an increased integration of power-electronics inverters serving as grid interfaces to renewable resources, electrical vehicles, and loads. For instance, today there are roughly 800,000 Enphase microinverters on the Hawaiian island of Oahu alone [1] and this number will only grow as Hawaii aims to meet its goal of obtaining 100% of its energy from renewable sources by 2045 [2]. To aid analysis and control, it is critical to develop computationally affordable models that scale with penetration level and accurately capture pertinent dynamics of power electronics inverters. This paper takes a step in this direction by formulating a reduced-order model for a collection of parallel-connected grid-tied three-phase inverters as may be seen in photovoltaic energy conversion systems, electric-vehicle charging stations, and railway auxiliary power supplies [3]–[5].

Without loss of generality, we examine a three-phase inverter with a full-bridge topology and output LCL filter. As shown in Fig. 1a, the inverter control system includes: a current controller (that generates the PWM reference signals), a power controller (that responds to active- and reactive-power setpoints and generates current references for the current controller), and a phase-locked loop (PLL) (for grid synchronization) [6]. Models of this sort generally have more than 10 dynamical states (the particular one we study has 15); and therefore, it is computationally infeasible and analytically unwieldy to study large collections of such inverters with different power ratings. To address these limitations, we derive a structure-preserving reduced-order inverter model for the setting where individual inverters in the parallel setup have the same topology with filter components and controller gains that scale linearly with the power rating. By structure preserving, we mean that the reduced-order model itself is a three-phase inverter that is also composed of an LCL filter, a power controller, current controller, and PLL, i.e., it has the same structure and the same number of dynamical states as any individual inverter in the parallel multi-inverter system.

Model-reduction methods for individual inverters and synchronous machines have received attention in the literature [7]–[9]. While model-reduction methods to analyze the collective dynamics of machines and droop-controlled islanded inverters have received attention [10], [11], this work focuses on large collections of the most ubiquitous type of inverter installed on systems today–grid-tied inverters with conventional grid-following current controllers and PLLs. We anticipate the models developed here to be applicable in such problems as the study of dynamic interactions between machines and inverters, as well as stability analysis of networks with high inverter penetration [12]–[14].

The remainder of this paper is organized as follows. In Section II, we introduce a three-phase grid-connected inverter model and power scaling laws for the inverter. In Section III, we describe how the states of the inverter are scaled based on its power-scaling parameter, and propose the reduced-order structure-preserving model for parallel-connected inverters. To validate the proposed reduced-order model, we compare numerical simulation of a parallel system to its corresponding reduced-order inverter in Section IV. Finally, we conclude this paper and outline a few pertinent directions for future work in Section V.

This work was supported by the U.S. Department of Energy (DOE) Solar Energy Technologies Office under Contract No. DE-EE0000-1583.

978-1-5090-5326-1/17/$31.00 ©2017 IEEE

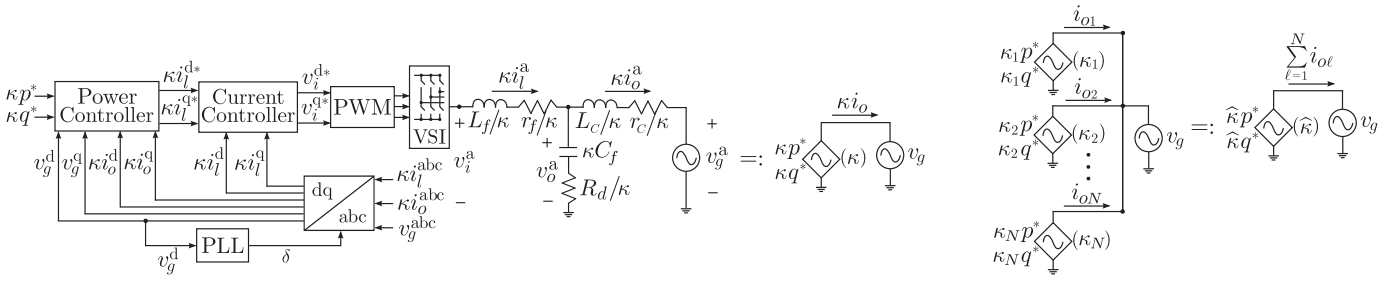

Fig. 1: (a) Block diagram of the three phase inverter (one leg of the LCL filter is depicted) and adopted shorthand. (b) For the parallel connection of N inverters we obtain the power-scaling parameter, $\widehat{\kappa}$, for a reduced-order structure-preserving model.

Notation: The matrix transpose will be denoted by $(\cdot)^{\mathrm{T}}$. The spaces of $N \times 1$ real-valued vectors is denoted by $\mathbb{R}^N$; and $\mathbb{R}^{N\times N}$ denotes the space of $N \times N$ real-valued matrices. A diagonal matrix formed with diagonal entries composed of entries of the vector x is denoted by $\mathrm{diag}(x)$; $\mathbb{1}_n$ and $\mathbb{0}_n$ denote an all ones and all zeros vectors of length n, respectively; I_n denotes an n-by-n identity matrix; $\mathbb{0}_{m\times n}$ denotes an all zeros matrix of size m-by-n.

II. The Inverter Model and Power Scaling Laws

A block diagram of the three-phase inverter is illustrated in Figure 1a. We assume a voltage source inverter (VSI) with an H-bridge topology and an output LCL filter (L_f, C_f, L_c). The grid voltage and frequency are denoted by v_g and ω_g, respectively. The control architecture for each inverter includes: an inner-loop current controller, an outer-loop power controller, and a phase-locked loop (for grid synchronization). As shown in Fig. 1b, we are primarily interested in the collective behavior of N such inverters connected in parallel to the grid. We begin this section with an overview on how the inverters are designed for different power ratings, the features of the reduced-order model sought for the parallel collection of inverters, and then briefly discuss the controller and LCL filter dynamics. Lastly, we represent the dynamics of the inverter in state-space form.

A. Scaling Individual Inverters with Power Rating

We first introduce the notion of a *power-scaling parameter*, κ, which is defined as

$$\kappa := \frac{p_{\mathrm{rated}}}{p_{\mathrm{base}}}, \tag{1}$$

where p_{rated} is the rated power of a given inverter, and p_{base} is a system-wide base value. We make the assumption that both real and reactive power ratings scale linearly with κ. In the remainder of the digest, we will denote the base active- and reactive-power setpoints as p^* and q^*. Notice from Fig. 1a that the reference-power setpoints for the inverter are given by $\kappa p^*, \kappa q^*$. Therefore, the output active and reactive power injected by each inverter into the grid are directly proportional to κ. We scale elements of the LCL filter in the manner shown in Fig. 1a so that the output current is inversely proportional to the impedance of the filter. With regard to the controllers, we also scale the gains of the current controller by $1/\kappa$ so that its outputs, i.e., the reference for the input voltage of the LCL filter, do not depend on κ, and neither does the voltage drop across the LCL filter. Thus, the output current, and therefore the output power, of the inverter scales directly proportionally to κ.

The scaling approach described above is admittedly assumptive by nature. However, it is a herculean—if not impossible—task to ascertain how commercial inverter manufacturers would scale the cyber-physical architectures of inverters with power rating. Therefore, we base our analysis around this scaling approach, taking solace in the fact that it is grounded in and guided by some fundamental engineering insights.

B. Desired Features of the Structure-preserving Reduced-order Model

With the control and physical architecture of individual inverters highlighted in Fig. 1a, and the procedure to scale the inverter design to accommodate different power ratings discussed above, we bring attention to Fig. 1b to describe the main goal of this work. We consider a collection of N inverters with different power ratings (described by power-scaling parameters $\kappa_1, \ldots, \kappa_N$) connected in parallel to the grid bus. The dynamics of each inverter include those of the different control blocks and LCL filters illustrated in Fig. 1a, and are described collectively by a 15-order model (which will be spelled out subsequently). We derive a structure-preserving reduced-order model for this parallel connection. Particularly, we will show that an inverter model with power-scaling parameter, $\widehat{\kappa} = \sum_{\ell=1}^{N} \kappa_\ell$ perfectly captures the input-output behavior of the N-inverter collection with a dynamical-system model that has the same order and structure as any individual inverter.

C. Model of an Individual Inverter

With the design procedure adopted for scaling inverters in place, and the goal of this effort described, we next briefly overview individual portions of the dynamical models for the individual inverters in Fig. 1a. We start with the reference-frame transformation, and then go through the phase-locked loop (PLL), the current controller, and the power controller. In

each case, we describe the model assuming assuming $\kappa = 1$, but indicate how the dynamics are modified for an inverter with a power rating that is not the base value.

1) Reference-frame transformation: Sinusoidally varying three-phase signals $(x^{\mathrm{a}}, x^{\mathrm{b}}, x^{\mathrm{c}})$ in balanced settings are coordinate transformed to equivalent DC signals $(x^{\mathrm{d}}, x^{\mathrm{q}})$ using Park's transformation:

$$\begin{bmatrix} x^{\mathrm{d}} \\ x^{\mathrm{q}} \end{bmatrix} = \frac{2}{3} \begin{bmatrix} \cos(\delta) & \cos(\delta - \frac{2\pi}{3}) & \cos(\delta + \frac{2\pi}{3}) \\ -\sin(\delta) & -\sin(\delta - \frac{2\pi}{3}) & -\sin(\delta + \frac{2\pi}{3}) \end{bmatrix} \begin{bmatrix} x^{\mathrm{a}} \\ x^{\mathrm{b}} \\ x^{\mathrm{c}} \end{bmatrix} =: \frac{2}{3} \Psi \begin{bmatrix} x^{\mathrm{a}} \\ x^{\mathrm{b}} \\ x^{\mathrm{c}} \end{bmatrix}, \tag{2}$$

where δ is the instantaneous angle generated by the PLL. The change in coordinates is signified with the *abc-dq* block in Fig. 1a. We further note that $[x^{\mathrm{a}}, x^{\mathrm{b}}, x^{\mathrm{c}}]^{\mathrm{T}} = \Psi^{\mathrm{T}}[x^{\mathrm{d}}, x^{\mathrm{q}}]^{\mathrm{T}}$. To illustrate the adopted notation in abc and dq coordinates, consider the grid voltage, v_g, without loss of generality. First, $v_g^{\mathrm{abc}} := [v_g^{\mathrm{a}}, v_g^{\mathrm{b}}, v_g^{\mathrm{c}}]^{\mathrm{T}}$ captures v_g in abc coordinates. In the dq reference frame, we define $v_g^{\mathrm{dq}} := [v_g^{\mathrm{d}}, v_g^{\mathrm{q}}]^{\mathrm{T}}$, and $v_g^{\mathrm{abc}} = \Psi^{\mathrm{T}} v_g^{\mathrm{dq}}$.

2) Phase-locked Loop: The PLL is in feedback with the dq transformation for the grid voltage, and it modulates the angle δ such that $v_g^{\mathrm{d}} \to 0$ asymptotically. (Elementary trigonometric identities coupled with (2) illustrate that when $v_g^{\mathrm{d}} = 0$, δ is the instantaneous phase angle of v_g^{a}, i.e., the inverter is *phase locked* with the grid.) It consists of a low pass filter (with cut-off frequency $\omega_{c,\mathrm{PLL}}$) and a PI controller (with PI gains k^p_{PLL} and k^i_{PLL}). The dynamics of the PLL that generate the angle δ are given by

$$\begin{aligned} \dot{v}_{\mathrm{PLL}} &= \omega_{c,\mathrm{PLL}}(v_g^{\mathrm{d}} - v_{\mathrm{PLL}}), \\ \dot{\phi}_{\mathrm{PLL}} &= -v_{\mathrm{PLL}}, \\ \dot{\delta} &= 2\pi \times 60 - k^p_{\mathrm{PLL}} v_{\mathrm{PLL}} + k^i_{\mathrm{PLL}} \phi_{\mathrm{PLL}} =: \omega_{\mathrm{PLL}}. \end{aligned} \tag{3}$$

From the dynamics, we can see that at steady state, $v_g^{\mathrm{d}} = v_{\mathrm{PLL}} = 0$. Furthermore, when the grid frequency, $\omega_g = 2\pi \times 60\,[\mathrm{rad} \cdot \mathrm{sec}^{-1}]$, it follows that $\dot{\delta} = \omega_{\mathrm{PLL}} = 2\pi \times 60\,[\mathrm{rad} \cdot \mathrm{sec}^{-1}]$.

Remark 1 (Dynamics of PLL in scaled inverter). The same dynamics in (3) are utilized for inverters with different power ratings, i.e., for the case $\kappa \neq 1$.

3) Output LCL Filter: The dynamics of the LCL filter (in the dq reference frame) are derived by running pertinent time-domain circuit equations through the dq transformation with angle δ. This yields

$$\begin{aligned} \dot{i}_l^{\mathrm{dq}} &= \frac{1}{L_f}(-r_f i_l^{\mathrm{dq}} + v_i^{\mathrm{dq}} - v_o^{\mathrm{dq}}) + \begin{bmatrix} 0 & 1 \\ -1 & 0 \end{bmatrix} \omega_{\mathrm{PLL}} i_l^{\mathrm{dq}}, \\ \dot{i}_o^{\mathrm{dq}} &= \frac{1}{L_c}(-r_c i_o^{\mathrm{dq}} + v_o^{\mathrm{dq}} - v_g^{\mathrm{dq}}) + \begin{bmatrix} 0 & 1 \\ -1 & 0 \end{bmatrix} \omega_{\mathrm{PLL}} i_o^{\mathrm{dq}}, \\ \dot{v}_o^{\mathrm{dq}} &= R_d(\dot{i}_l^{\mathrm{dq}} - \dot{i}_o^{\mathrm{dq}}) - \begin{bmatrix} 0 & 1 \\ -1 & 0 \end{bmatrix} \omega_{\mathrm{PLL}} R_d(i_l^{\mathrm{dq}} - i_o^{\mathrm{dq}}) \\ &\quad + \frac{1}{C_f}(i_l^{\mathrm{dq}} - i_o^{\mathrm{dq}}) + \begin{bmatrix} 0 & 1 \\ -1 & 0 \end{bmatrix} \omega_{\mathrm{PLL}} v_o^{\mathrm{dq}}, \end{aligned} \tag{4}$$

where $i_l^{\mathrm{dq}} = [i_l^{\mathrm{d}}, i_l^{\mathrm{q}}]^{\mathrm{T}}$, $i_o^{\mathrm{dq}} = [i_o^{\mathrm{d}}, i_o^{\mathrm{q}}]^{\mathrm{T}}$, $v_i^{\mathrm{dq}} = [v_i^{\mathrm{d}}, v_i^{\mathrm{q}}]^{\mathrm{T}}$, and $v_o^{\mathrm{dq}} = [v_o^{\mathrm{d}}, v_o^{\mathrm{q}}]^{\mathrm{T}}$.

Remark 2 (Dynamics of LCL filter in scaled inverter). While the dynamics above correspond to the case where the power-scaling parameter, $\kappa = 1$; for inverters with power ratings that are scaled values of this base setting, we utilize the filter parameters L_f/κ, r_f/κ, κC_f, R_d/κ, L_c/κ, r_c/κ with κ chosen according to (1).

4) Power Controller: The power controller consists of low pass filters and PI controllers, with its outputs to be the reference for the current controller:

$$\begin{aligned} i_l^{\mathrm{d}*} &= k_Q^p\,(q^* - q_{\mathrm{avg}}) + k_Q^i \int q^* - q_{\mathrm{avg}}, \\ i_l^{\mathrm{q}*} &= k_P^p\,(p^* - p_{\mathrm{avg}}) + k_P^i \int p^* - p_{\mathrm{avg}}, \end{aligned}$$

where p^*, q^* are reference active- and reactive-power setpoints. Furthermore, p_{avg} and q_{avg} are low-pass-filtered versions of the inverter output active and reactive power outputs:

$$\dot{p}_{\mathrm{avg}} = \omega_c(p - p_{\mathrm{avg}}), \quad \dot{q}_{\mathrm{avg}} = \omega_c(q - q_{\mathrm{avg}}), \tag{5}$$

where p and q are the instantaneous active and reactive output power (measured at the grid terminals) and given by

$$p = \frac{3}{2}(v_g^{\mathrm{d}} i_o^{\mathrm{d}} + v_g^{\mathrm{q}} i_o^{\mathrm{q}}), \quad q = \frac{3}{2}(v_g^{\mathrm{q}} i_o^{\mathrm{d}} - v_g^{\mathrm{d}} i_o^{\mathrm{q}}).$$

To ease notation and exposition in subsequent developments, we will find it useful to define:

$$\dot{\phi}_p := p^* - p_{\mathrm{avg}}, \quad \dot{\phi}_q := q^* - q_{\mathrm{avg}}. \tag{6}$$

Remark 3 (Dynamics of power controller in scaled inverter). For inverters with $\kappa \neq 1$, the power setpoints as scaled as κp^* and κq^*; all other dynamics reported above are retained.

5) Current Controller: The current controller consists of two PI controllers and feedforward terms, with its outputs to be the reference for the terminal voltage v_i:

$$\begin{aligned} v_i^{\mathrm{d}*} &= -\omega_{\mathrm{PLL}} L_f i_l^{\mathrm{q}} + k_{\mathrm{id}}^p \left(i_l^{\mathrm{d}*} - i_l^{\mathrm{d}}\right) + k_{\mathrm{id}}^i \int i_l^{\mathrm{d}*} - i_l^{\mathrm{d}}, \\ v_i^{\mathrm{q}*} &= \omega_{\mathrm{PLL}} L_f i_l^{\mathrm{d}} + k_{\mathrm{iq}}^p \left(i_l^{\mathrm{q}*} - i_l^{\mathrm{q}}\right) + k_{\mathrm{iq}}^i \int i_l^{\mathrm{q}*} - i_l^{\mathrm{q}}. \end{aligned}$$

To ease notation and exposition in subsequent developments, we will find it useful to define:

$$\dot{\gamma}^{\mathrm{d}} = i_l^{\mathrm{d}*} - i_l^{\mathrm{d}}, \quad \dot{\gamma}^{\mathrm{q}} = i_l^{\mathrm{q}*} - i_l^{\mathrm{q}}. \tag{7}$$

The (three-phase) PWM modulation signals for the inverter are then obtained as $v_i^{\mathrm{abc}*} = \Psi^{\mathrm{T}} v_i^{\mathrm{dq}*}$. With reference to Fig. 1a, for an ideal inverter we have that the inverter terminal voltage, $v_i^{\mathrm{abc}} = v_i^{\mathrm{abc}*}$ (and equivalently $v_i^{\mathrm{dq}} = v_i^{\mathrm{dq}*}$).

Remark 4 (Dynamics of current controller in scaled inverter). While the dynamics above correspond to the case where the power-scaling parameter, $\kappa = 1$; for inverters with power ratings that are scaled values of this base setting, we utilize the parameters k_{id}^p/κ, k_{iq}^p/κ, k_{id}^i/κ, k_{iq}^i/κ.

D. State-space Model for the Inverter Dynamics

For the model in (3)–(7), we assumed that $\kappa = 1$ and hence, it defines the dynamics in the *unscaled* inverter. For this case, the controller and LCL filter dynamics can be compactly represented in state-space form as follows

$$\dot{\underline{x}} = A\underline{x} + B\underline{u}_1 + g(\underline{x}, \underline{u}_2), \tag{8}$$

where the states are $\underline{x} = [i_l^{\mathrm{d}}, i_l^{\mathrm{q}}, i_o^{\mathrm{d}}, i_o^{\mathrm{q}}, \gamma^{\mathrm{d}}, \gamma^{\mathrm{q}}, p_{\mathrm{avg}}, q_{\mathrm{avg}}, \phi_p, \phi_q, v_o^{\mathrm{d}}, v_o^{\mathrm{q}}, v_{\mathrm{PLL}}, \phi_{\mathrm{PPL}}, \delta]^{\mathrm{T}}$, and the inputs include $\underline{u}_1 = [p^*, q^*]^{\mathrm{T}}$ and $\underline{u}_2 = [v_g^{\mathrm{a}}, v_g^{\mathrm{b}}, v_g^{\mathrm{c}}]^{\mathrm{T}} = v_g^{\mathrm{abc}}$. Here, the matrices $A \in \mathbb{R}^{15\times 15}$, $B \in \mathbb{R}^{15\times 2}$, and function $g : \mathbb{R}^{15} \times \mathbb{R}^3 \to \mathbb{R}^{15}$ can be derived from the dynamical-system models in (6)–(7) straightforwardly. For completeness, their entries are listed in the Appendix.

Now, let us consider a *scaled* inverter with $\kappa \neq 1$. If we replace the unscaled model parameters $L_f, r_f, C_f, R_d, L_c, r_c, k_{\mathrm{id}}^p, k_{\mathrm{iq}}^p, k_{\mathrm{id}}^i, k_{\mathrm{id}}^i$ with $\kappa^{-1}L_f, \kappa^{-1}r_f, \kappa C_f, \kappa^{-1}R_d, \kappa^{-1}L_c, \kappa^{-1}r_c, \kappa^{-1}k_{\mathrm{id}}^p, \kappa^{-1}k_{\mathrm{iq}}^p$, $\kappa^{-1}k_{\mathrm{id}}^i, \kappa^{-1}k_{\mathrm{iq}}^i$ (see Remark 1–4), we obtain the *scaled* inverter model

$$\dot{\underline{x}}^{\mathrm{s}} = A^{\mathrm{s}}\underline{x}^{\mathrm{s}} + B^{\mathrm{s}}\underline{u}_1^{\mathrm{s}} + g^{\mathrm{s}}(\underline{x}^{\mathrm{s}}, \underline{u}_2^{\mathrm{s}}), \tag{9}$$

where the inputs are $\underline{u}_1^{\mathrm{s}} = \kappa\underline{u}_1$ and $\underline{u}_2^{\mathrm{s}} = \underline{u}_2 = v_g^{\mathrm{abc}}$. The matrices $A^{\mathrm{s}} \in \mathbb{R}^{15\times 15}$, $B^{\mathrm{s}} \in \mathbb{R}^{15\times 2}$, and function $g^{\mathrm{s}} : \mathbb{R}^{15} \times \mathbb{R}^3 \to \mathbb{R}^{15}$ have the same structure as A, B, and g for the unscaled model albeit with parametric scalings given above. Next, define $\underline{\kappa} := [\kappa\mathbb{1}_{10}^{\mathrm{T}}, \mathbb{1}_5^{\mathrm{T}}]^{\mathrm{T}}$, where $\mathbb{1}_\ell$ denotes an ℓ-length vector of all ones.

III. Inverter Scaling and Reduced-order Model

In this section, we begin with establishing the relationship between the states in the scaled and unscaled inverter models, then we propose a method of aggregating N parallel-connected inverters illustrated in Fig. 1b.

A. Scaling of Inverter States

Here, we establish the connection between the dynamics of the scaled and unscaled inverters.

Proposition 1. Consider the dynamics of the unscaled inverter (with $\kappa = 1$) and scaled inverter (with $\kappa \neq 1$) in (8) and (9), respectively. Suppose the initial conditions for the two dynamical systems at some time $t_0 \geq 0$ are such that $\underline{x}^{\mathrm{s}}(t_0) = \mathrm{diag}(\underline{\kappa})\underline{x}(t_0)$. If $\underline{u}_1^{\mathrm{s}} = \kappa\underline{u}_1$ and $\underline{u}_2^{\mathrm{s}} = \underline{u}_2$, it follows that $\underline{x}^{\mathrm{s}}(t) = \mathrm{diag}(\underline{\kappa})\underline{x}(t),\ \forall t \geq t_0$.

Proof. We partition $\underline{x}$ as $[\underline{x}_1^{\mathrm{T}}, \underline{x}_2^{\mathrm{T}}]^{\mathrm{T}}$, where $\underline{x}_1^{\mathrm{T}} = [i_l^{\mathrm{d}}, i_l^{\mathrm{q}}, i_o^{\mathrm{d}}, i_o^{\mathrm{q}}, \gamma^{\mathrm{d}}, \gamma^{\mathrm{q}}, p_{\mathrm{avg}}, q_{\mathrm{avg}}, \phi_p, \phi_q]^{\mathrm{T}}$ and $\underline{x}_2^{\mathrm{T}} = [v_o^{\mathrm{d}}, v_o^{\mathrm{q}}, v_{\mathrm{PLL}}, \phi_{\mathrm{PPL}}, \delta]^{\mathrm{T}}$, and we also partition $\underline{x}^{\mathrm{s}}$ the same way. Then we write (8) and (9) as follows

$$\begin{bmatrix}\dot{\underline{x}}_1\\ \dot{\underline{x}}_2\end{bmatrix} = \begin{bmatrix}A_{11} & A_{12}\\ A_{21} & A_{22}\end{bmatrix}\begin{bmatrix}\underline{x}_1\\ \underline{x}_2\end{bmatrix} + \begin{bmatrix}B_1\\ B_2\end{bmatrix}\underline{u}_1 + g(\underline{x}, \underline{u}_2), \tag{10}$$

$$\begin{bmatrix}\dot{\underline{x}}_1^{\mathrm{s}}\\ \dot{\underline{x}}_2^{\mathrm{s}}\end{bmatrix} = \begin{bmatrix}A_{11}^{\mathrm{s}} & A_{12}^{\mathrm{s}}\\ A_{21}^{\mathrm{s}} & A_{22}^{\mathrm{s}}\end{bmatrix}\begin{bmatrix}\underline{x}_1^{\mathrm{s}}\\ \underline{x}_2^{\mathrm{s}}\end{bmatrix} + \begin{bmatrix}B_1^{\mathrm{s}}\\ B_2^{\mathrm{s}}\end{bmatrix}\underline{u}_1^{\mathrm{s}} + g^{\mathrm{s}}(\underline{x}^{\mathrm{s}}, \underline{u}_2^{\mathrm{s}}). \tag{11}$$

By observing the entries of the state-space matrices, it is straightforward to see the following relationships:

$$A_{11}^{\mathrm{s}} = A_{11},\ A_{12}^{\mathrm{s}} = \kappa A_{12},\ A_{21}^{\mathrm{s}} = \frac{1}{\kappa}A_{21},\ A_{22}^{\mathrm{s}} = A_{22},$$

$$B_1^{\mathrm{s}} = B_1,\ B_2^{\mathrm{s}} = \frac{1}{\kappa}B_2.$$

Then we have

$$\mathrm{diag}(\underline{\kappa})A = \begin{bmatrix}\kappa A_{11} & \kappa A_{12}\\ A_{21} & A_{22}\end{bmatrix} = \begin{bmatrix}\kappa A_{11}^{\mathrm{s}} & A_{12}^{\mathrm{s}}\\ \kappa A_{21}^{\mathrm{s}} & A_{22}^{\mathrm{s}}\end{bmatrix} = A^{\mathrm{s}}\mathrm{diag}(\underline{\kappa}), \tag{12}$$

$$\mathrm{diag}(\underline{\kappa})B = \begin{bmatrix}\kappa B_1\\ B_2\end{bmatrix} = \begin{bmatrix}\kappa B_1^{\mathrm{s}}\\ \kappa B_2^{\mathrm{s}}\end{bmatrix} = B^{\mathrm{s}}(\kappa \mathrm{I}_2). \tag{13}$$

Next, we are going to show that $g^{\mathrm{s}}(\mathrm{diag}(\underline{\kappa})\underline{x}, \underline{u}_2^{\mathrm{s}}) = \mathrm{diag}(\underline{\kappa})g(\underline{x}, \underline{u}_2)$. Notice that the PLL dynamics for both inverters are decoupled from the rest of internal states and their parameters are the same, so we can conclude that $v_g^{\beta\mathrm{s}} = v_g^{\beta}, v_{\mathrm{PLL}}^{\mathrm{s}} = v_{\mathrm{PLL}}, \phi_{\mathrm{PLL}}^{\mathrm{s}} = \phi_{\mathrm{PLL}}, \delta^{\mathrm{s}} = \delta$. Then, the following identities hold for v_g^{d} and v_g^{q}:

$$\begin{aligned} v_g^{\mathrm{d}}(\mathrm{diag}(\underline{\kappa})\underline{x}, \underline{u}_2^{\mathrm{s}}) &= \frac{2}{3}\Big(\cos(\delta)v_g^{\mathrm{a}} + \cos(\delta - \frac{2\pi}{3})v_g^{\mathrm{b}} \\ &\quad + \cos(\delta + \frac{2\pi}{3})v_g^{\mathrm{c}}\Big) = v_g^{\mathrm{d}}(\underline{x}, \underline{u}_2^{\mathrm{s}}) = v_g^{\mathrm{d}}(\underline{x}, \underline{u}_2),\\ v_g^{\mathrm{q}}(\mathrm{diag}(\underline{\kappa})\underline{x}, \underline{u}_2^{\mathrm{s}}) &= \frac{2}{3}\Big(\sin(\delta)v_g^{\mathrm{a}} + \sin(\delta - \frac{2\pi}{3})v_g^{\mathrm{b}} \\ &\quad + \sin(\delta + \frac{2\pi}{3})v_g^{\mathrm{c}}\Big) = v_g^{\mathrm{q}}(\underline{x}, \underline{u}_2^{\mathrm{s}}) = v_g^{\mathrm{q}}(\underline{x}, \underline{u}_2). \end{aligned}$$

The nonzero entries of $g^{\mathrm{s}}(\mathrm{diag}(\underline{\kappa})\underline{x}, \underline{u}_2^{\mathrm{s}})$ are given by

$$\begin{aligned} g_3^{\mathrm{s}}(\mathrm{diag}(\underline{\kappa})\underline{x}, \underline{u}_2^{\mathrm{s}}) &= (-k_{\mathrm{PLL}}^p v_{\mathrm{PLL}} + k_{\mathrm{PLL}}^i\phi_{\mathrm{PLL}})\kappa i_o^{\mathrm{q}} \\ &\quad - \frac{\kappa}{L_c}v_g^{\mathrm{d}}(\mathrm{diag}(\underline{\kappa})\underline{x}, \underline{u}_2^{\mathrm{s}}) = \kappa g_3(\underline{x}, \underline{u}_2^{\mathrm{s}}),\\ g_4^{\mathrm{s}}(\mathrm{diag}(\underline{\kappa})\underline{x}, \underline{u}_2^{\mathrm{s}}) &= (k_{\mathrm{PLL}}^p v_{\mathrm{PLL}} - k_{\mathrm{PLL}}^i\phi_{\mathrm{PLL}})\kappa i_o^{\mathrm{d}} \\ &\quad - \frac{\kappa}{L_c}v_g^{\mathrm{q}}(\mathrm{diag}(\underline{\kappa})\underline{x}, \underline{u}_2^{\mathrm{s}}) = \kappa g_4(\underline{x}, \underline{u}_2^{\mathrm{s}}),\\ g_7^{\mathrm{s}}(\mathrm{diag}(\underline{\kappa})\underline{x}, \underline{u}_2^{\mathrm{s}}) &= \frac{3}{2}\kappa\omega_c\left(v_g^{\mathrm{d}}(\mathrm{diag}(\underline{\kappa})\underline{x}, \underline{u}_2^{\mathrm{s}})i_o^{\mathrm{d}}\right.\\ &\quad \left. + v_g^{\mathrm{q}}(\mathrm{diag}(\underline{\kappa})\underline{x}, \underline{u}_2^{\mathrm{s}})i_o^{\mathrm{q}}\right) = \kappa g_7(\underline{x}, \underline{u}_2^{\mathrm{s}}),\\ g_8^{\mathrm{s}}(\mathrm{diag}(\underline{\kappa})\underline{x}, \underline{u}_2^{\mathrm{s}}) &= \frac{3}{2}\kappa\omega_c\left(v_g^{\mathrm{q}}(\mathrm{diag}(\underline{\kappa})\underline{x}, \underline{u}_2^{\mathrm{s}})i_o^{\mathrm{d}}\right.\\ &\quad \left. - v_g^{\mathrm{d}}(\mathrm{diag}(\underline{\kappa})\underline{x}, \underline{u}_2^{\mathrm{s}})i_o^{\mathrm{q}}\right) = \kappa g_8(\underline{x}, \underline{u}_2^{\mathrm{s}}),\\ g_{11}^{\mathrm{s}}(\mathrm{diag}(\underline{\kappa})\underline{x}, \underline{u}_2^{\mathrm{s}}) &= (-k_{\mathrm{PLL}}^p v_{\mathrm{PLL}} + k_{\mathrm{PLL}}^i\phi_{\mathrm{PLL}})(-R_d i_l^{\mathrm{q}} + v_o^{\mathrm{q}}) \\ &\quad + \frac{R_d}{L_c}v_g^{\mathrm{d}}(\mathrm{diag}(\underline{\kappa})\underline{x}, \underline{u}_2^{\mathrm{s}}) = g_{11}(\underline{x}, \underline{u}_2^{\mathrm{s}}),\\ g_{12}^{\mathrm{s}}(\mathrm{diag}(\underline{\kappa})\underline{x}, \underline{u}_2^{\mathrm{s}}) &= (k_{\mathrm{PLL}}^p v_{\mathrm{PLL}} - k_{\mathrm{PLL}}^i\phi_{\mathrm{PLL}})(-R_d i_l^{\mathrm{d}} + v_o^{\mathrm{d}}) \\ &\quad + \frac{R_d}{L_c}v_g^{\mathrm{q}}(\mathrm{diag}(\underline{\kappa})\underline{x}, \underline{u}_2^{\mathrm{s}}) = g_{12}(\underline{x}, \underline{u}_2^{\mathrm{s}}),\\ g_{13}^{\mathrm{s}}(\mathrm{diag}(\underline{\kappa})\underline{x}, \underline{u}_2^{\mathrm{s}}) &= \omega_{c,\mathrm{PLL}}v_g^{\mathrm{d}}(\underline{x}, \underline{u}_2) = g_{13}(\underline{x}, \underline{u}_2^{\mathrm{s}}),\\ g_{15}^{\mathrm{s}}(\mathrm{diag}(\underline{\kappa})\underline{x}, \underline{u}_2^{\mathrm{s}}) &= 2\pi \times 60 = g_{15}(\underline{x}, \underline{u}_2^{\mathrm{s}}), \underline{u}_2). \end{aligned}$$

Therefore, we have

$$\mathrm{diag}(\underline{\kappa})g(\underline{x}, \underline{u}_2) = g^{\mathrm{s}}(\mathrm{diag}(\underline{\kappa})\underline{x}, \underline{u}_2^{\mathrm{s}}). \tag{14}$$

Let us define function $h(\underline{x}^{\mathrm{s}}, \underline{u}_2^{\mathrm{s}}) : \mathbb{R}^{15} \times \mathbb{R}^2 \to \mathbb{R}^{15}$ to have the same structure as $g^{\mathrm{s}}(\underline{x}^{\mathrm{s}}\underline{u}_2^{\mathrm{s}})$ except the following entries:

$$h_3(\underline{x}^{\mathrm{s}}, \underline{u}_2^{\mathrm{s}}) = (-k^p_{\mathrm{PLL}} v^{\mathrm{s}}_{\mathrm{PLL}} + k^i_{\mathrm{PLL}} \phi^{\mathrm{s}}_{\mathrm{PLL}}) i_o^{\mathrm{qs}},$$
$$h_4(\underline{x}^{\mathrm{s}}, \underline{u}_2^{\mathrm{s}}) = (k^p_{\mathrm{PLL}} v^{\mathrm{s}}_{\mathrm{PLL}} - k^i_{\mathrm{PLL}} \phi^{\mathrm{s}}_{\mathrm{PLL}}) i_o^{\mathrm{ds}},$$
$$h_{11}(\underline{x}^{\mathrm{s}}, \underline{u}_2^{\mathrm{s}}) = (-k^p_{\mathrm{PLL}} v^{\mathrm{s}}_{\mathrm{PLL}} + k^i_{\mathrm{PLL}} \phi^{\mathrm{s}}_{\mathrm{PLL}}) \left(-\frac{R_d}{\kappa} i_l^{\mathrm{qs}} + v_o^{\mathrm{qs}} \right),$$
$$h_{12}(\underline{x}^{\mathrm{s}}, \underline{u}_2^{\mathrm{s}}) = (k^p_{\mathrm{PLL}} v^{\mathrm{s}}_{\mathrm{PLL}} - k^i_{\mathrm{PLL}} \phi^{\mathrm{s}}_{\mathrm{PLL}}) \left(-\frac{R_d}{\kappa} i_l^{\mathrm{ds}} + v_o^{\mathrm{ds}} \right),$$
$$h_{13}(\underline{x}^{\mathrm{s}}, \underline{u}_2^{\mathrm{s}}) = 0,$$
$$h_{15}(\underline{x}^{\mathrm{s}}, \underline{u}_2^{\mathrm{s}}) = 0.$$

Then, the following identity holds

$$g^{\mathrm{s}}(\underline{x}^{\mathrm{s}}, \underline{u}_2^{\mathrm{s}}) - g^{\mathrm{s}}(\mathrm{diag}(\underline{\kappa})\underline{x}, \underline{u}_2^{\mathrm{s}}) = h((\underline{x}^{\mathrm{s}} - \mathrm{diag}\,(\underline{\kappa})\underline{x}), \underline{u}_2^{\mathrm{r}})\,. \tag{15}$$

Let us define $\underline{z} := \underline{x}^{\mathrm{s}} - \mathrm{diag}(\underline{\kappa})\underline{x}$, and note from (10) and (11) that

$$\begin{aligned}\dot{\underline{z}} = \dot{\underline{x}}^{\mathrm{s}} - \mathrm{diag}(\underline{\kappa})\dot{\underline{x}} &= A^{\mathrm{s}}\underline{x}^{\mathrm{s}} + B^{\mathrm{s}}\underline{u}_1^{\mathrm{s}} + g^{\mathrm{s}}(\underline{x}^{\mathrm{s}}, \underline{u}_2^{\mathrm{s}}) \\ &\quad - \mathrm{diag}(\underline{\kappa})A\underline{x} - \mathrm{diag}(\underline{\kappa})B\underline{u}_1 - \mathrm{diag}(\underline{\kappa})g(\underline{x}, \underline{u}_2). \end{aligned} \tag{16}$$

Leveraging identities (12)–(15), we can rewrite (16) as

$$\begin{aligned}\dot{\underline{z}} &= A^{\mathrm{s}}(\underline{x}^{\mathrm{s}} - \mathrm{diag}(\underline{x})) + h((\underline{x}^{\mathrm{s}} - \mathrm{diag}\,(\underline{\kappa})\underline{x}), \underline{u}_2^{\mathrm{s}}) \\ &= A^{\mathrm{s}}\underline{z} + h(\underline{z}, \underline{u}_2^{\mathrm{s}}). \end{aligned} \tag{17}$$

It is straightforward to see $h(\mathbb{0}_{15}, \underline{u}_2^{\mathrm{s}}) = \mathbb{0}_{15}$. Then, if we initialize $\underline{z}(t_0) = \underline{x}^{\mathrm{s}}(t_0) - \mathrm{diag}(\underline{\kappa})\underline{x}(t_0) = \mathbb{0}_{15}$, we have $\underline{z}(t) = \mathbb{0}_{15}, \forall t \geq t_0$. Therefore we have $\underline{x}^{\mathrm{s}}(t) = \mathrm{diag}(\underline{\kappa})\underline{x}(t), \forall t \geq t_0$. □

B. Aggregation of Inverters

Consider the parallel-connection of N inverters with power-scaling factors $\kappa_1, \ldots, \kappa_N$ illustrated in Fig. 1b. Define the equivalent power-scaling factor as $\widehat{\kappa} := \sum_{\ell=1}^{N} \kappa_\ell$. For this system, define the reduced-order model

$$\dot{\underline{x}}^{\mathrm{r}} = A^{\mathrm{r}}\underline{x}^{\mathrm{r}} + B^{\mathrm{r}}\underline{u}_1^{\mathrm{r}} + g^{\mathrm{r}}(\underline{x}^{\mathrm{r}}, \underline{u}_2^{\mathrm{r}}), \tag{18}$$

where the inputs $\underline{u}_1^{\mathrm{r}}$ and $\underline{u}_2^{\mathrm{r}}$ are given by $\underline{u}_1^{\mathrm{r}} = \widehat{\kappa}[p^*, q^*]^{\mathrm{T}}$, $\underline{u}_2^{\mathrm{r}} = [v_g^{\mathrm{a}}, v_g^{\mathrm{b}}, v_g^{\mathrm{c}}]^{\mathrm{T}} = v_g^{\mathrm{abc}}$, and we have the same collection of states as the model in (9), except with the dynamics of the states being governed with $\kappa = \widehat{\kappa}$. Consequently, $A^{\mathrm{r}} \in \mathbb{R}^{15\times 15}$, $B^{\mathrm{r}} \in \mathbb{R}^{15\times 2}$, $g^{\mathrm{r}} : \mathbb{R}^{15} \times \mathbb{R}^3 \to \mathbb{R}^{15}$ have the same structure as (9), except with power-scaling parameter $\widehat{\kappa}$.

Proposition 2. Let $i_{o\ell}^{\mathrm{d}}$ and $i_{o\ell}^{\mathrm{q}}$ denote the output current of the ℓ-th inverter. Then, the output current of the reduced-order inverter is given by

$$i_o^{\mathrm{dr}}(t) = \sum_{\ell=1}^{N} i_{o\ell}^{\mathrm{d}}, \quad i_o^{\mathrm{qr}}(t) = \sum_{\ell=1}^{N} i_{o\ell}^{\mathrm{q}}, \tag{19}$$

where i_o^{dr} and i_o^{qr} denote the output current of the reduced-order inverter.

Proof. Let i_o^{d0} and i_o^{q0} denote the current output of inverter with nominal power rating. Since the reduced-order inverter has power-scaling factor of $\widehat{\kappa}$, $i_o^{\mathrm{dr}}(t) = \widehat{\kappa} i_o^{\mathrm{d0}}(t)$ and $i_o^{\mathrm{qr}}(t) = \widehat{\kappa} i_o^{\mathrm{q0}}(t)$ for $t \geq t_0$. By the definition of $\widehat{\kappa}$ and the scaling of output current, the following equations hold for $t \geq t_0$:

$$i_o^{\mathrm{dr}}(t) = \widehat{\kappa} i_o^{\mathrm{d0}}(t) = \sum_{\ell=1}^{N} \kappa_\ell i_o^{\mathrm{d0}}(t) = \sum_{\ell=1}^{N} i_{o\ell}^{\mathrm{d}}(t),$$

and similarly for the q component of the current. □

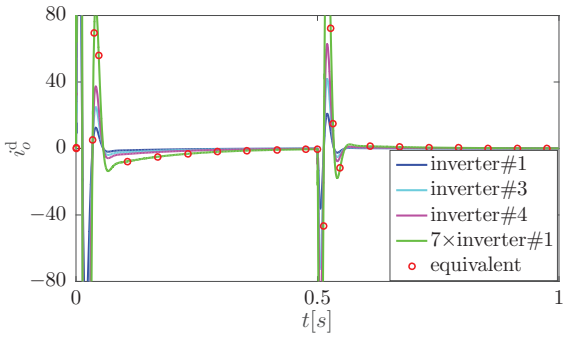

(a) d-axis output current

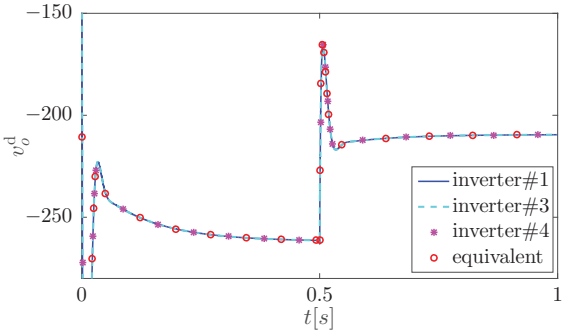

(b) d-axis output voltage

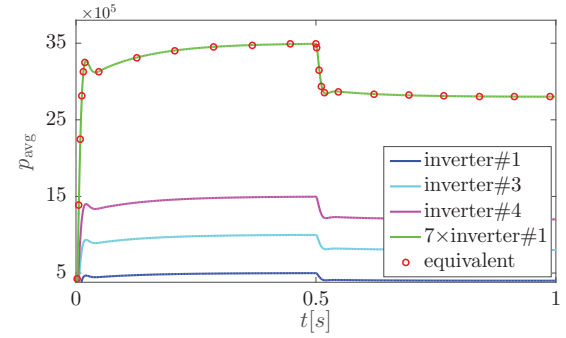

(c) Output power

Fig. 2: Simulation results for three-phase inverter system demonstrating the validity of the scaling and model-reduction procedure.

IV. Simulation Results

In this section, we simulate a system of 4 parallel-connected inverters alongside the reduced-order equivalent inverter model, as illustrated in Fig. 1b. For the multi-inverter system, $N = 4$, with power-scaling parameters: $\kappa_1 = \kappa_2 = 1$, $\kappa_3 = 2$, and $\kappa_4 = 3$. The reduced-order inverter model is given initial conditions as prescribed in Proposition 2. The power and RMS voltage ratings are 500kW and 288V, respectively,

and correspond to a Siemens SINVERT PVS500 inverter [15]. During the time-domain simulation, we let $q^* = 0$VAR. The filter and controller parameters are taken from [9]. We introduce a step change in p^* from 500kW to 400kW at $t = 0.5$s. Figure 2 shows the output current, voltage, and active power dynamics of the individual and equivalent (i.e. reduced-order) inverters. Note that the plots for inverter#2 are omitted since it has the same scaling factor as inverter#1, and therefore their plots are identical. To validate the equivalent inverter and its correspondence to the individual inverters, we also plot the output current and power of the unscaled inverter (i.e. inverter#1) scaled by a factor of 7. We can see that they satisfy the following scaling properties: $i_o^{\mathrm{dr}}(t) = 7i_{o1}^{\mathrm{d}}(t)$, $v_o^{\mathrm{dr}}(t) = v_{o1}^{\mathrm{d}}(t)$, and $p_{\mathrm{avg}}^{\mathrm{r}}(t) = 7p_{\mathrm{avg1}}(t)$.

V. Concluding Remarks and Directions for Future Work

In this paper, we derived a reduced-order structure-preserving model for parallel-connected grid-tied three-phase inverters. In particular, it was shown that N parallel inverters with heterogeneous power ratings can be modeled as a single inverter with an equivalent power rating equal to the sum of the individual inverter ratings. At its foundation, the proposed reduced order model is built on a set of scaling laws that prescribe how the filter and controller parameters of an individual inverter change with power rating. Ultimately, we showed that N parallel inverters that adhere to such scaling laws can be represented as one equivalent inverter whose output terminal behavior is identical to the original multi-inverter system. The next step of our study is to extend this result for the system of inverters with arbitrary electrical networks.

Appendix

In order to show the entries of matrices A, B, and function $g(\underline{x}, \underline{u}_2)$ compactly, let us permute the state vector as $\widehat{\underline{x}} := [i_l^{\mathrm{d}}, i_l^{\mathrm{q}}, i_o^{\mathrm{d}}, i_o^{\mathrm{q}}, v_o^{\mathrm{d}}, v_o^{\mathrm{q}}, \gamma^{\mathrm{d}}, \gamma^{\mathrm{q}}, p_{\mathrm{avg}}, q_{\mathrm{avg}}, \phi_p, \phi_q, v_{\mathrm{PLL}}, \phi_{\mathrm{PPL}}, \delta]^{\mathrm{T}}$, and the permuted dynamics are given by

$$\dot{\widehat{\underline{x}}} = \widehat{A}\widehat{\underline{x}} + \widehat{B}\underline{u}_1 + \widehat{g}(\widehat{\underline{x}}, \underline{u}_2), \tag{20}$$

Suppose we partition the permuted state vector as $\widehat{\underline{x}} = [\underline{x}_{LCL}^{\mathrm{T}}, \underline{x}_{\mathrm{CC}}^{\mathrm{T}}, \underline{x}_{\mathrm{PC}}^{\mathrm{T}}, \underline{x}_{\mathrm{PLL}}^{\mathrm{T}}]^{\mathrm{T}}$, where $\underline{x}_{LCL} = [i_l^{\mathrm{d}}, i_l^{\mathrm{q}}, i_o^{\mathrm{d}}, i_o^{\mathrm{q}}, v_o^{\mathrm{d}}, v_o^{\mathrm{q}}]^{\mathrm{T}}$, $\underline{x}_{\mathrm{CC}} = [\gamma^{\mathrm{d}}, \gamma^{\mathrm{q}}]^{\mathrm{T}}$, $\underline{x}_{\mathrm{PC}} = [p_{\mathrm{avg}}, q_{\mathrm{avg}}, \phi_p, \phi_q]^{\mathrm{T}}$, and $\underline{x}_{\mathrm{PLL}} = [v_{\mathrm{PLL}}, \phi_{\mathrm{PLL}}, \delta]^{\mathrm{T}}$. Then, we can write (20) as

$$\begin{bmatrix} \dot{\underline{x}}_{LCL} \\ \dot{\underline{x}}_{\mathrm{CC}} \\ \dot{\underline{x}}_{\mathrm{PC}} \\ \dot{\underline{x}}_{\mathrm{PLL}} \end{bmatrix} = \begin{bmatrix} A_{LCL} & A_{LCL}^{\mathrm{CC}} & A_{LCL}^{\mathrm{PC}} & \mathbb{0}_{6\times 3} \\ A_{\mathrm{CC}}^{LCL} & \mathbb{0}_{2\times 2} & A_{\mathrm{CC}}^{\mathrm{PC}} & \mathbb{0}_{2\times 3} \\ \mathbb{0}_{4\times 6} & \mathbb{0}_{4\times 2} & A_{\mathrm{PC}} & \mathbb{0}_{4\times 3} \\ \mathbb{0}_{4\times 6} & \mathbb{0}_{4\times 2} & \mathbb{0}_{4\times 4} & A_{\mathrm{PLL}} \end{bmatrix} \begin{bmatrix} \underline{x}_{LCL} \\ \underline{x}_{\mathrm{CC}} \\ \underline{x}_{\mathrm{PC}} \\ \underline{x}_{\mathrm{PLL}} \end{bmatrix} + \begin{bmatrix} B_{LCL} \\ B_{\mathrm{CC}} \\ B_{\mathrm{PC}} \\ 0_{3\times 2} \end{bmatrix} \underline{u}_1 + \widehat{g}(\widehat{\underline{x}}, \underline{u}_2),$$

where the nonzero submatrices A_{LCL}, A_{LCL}^{CC}, A_{LCL}^{PC}, A_{CC}^{LCL}, $A_{\mathrm{CC}}^{\mathrm{PC}}$, A_{PC}, A_{PLL}, B_{LCL}, B_{CC}, and B_{PC} are given by

$$A_{LCL} = \begin{bmatrix} -\frac{k_{\mathrm{id}}^p + r_f}{L_f} & 0 & 0 \\ 0 & -\frac{k_{\mathrm{id}}^p + r_f}{L_f} & 0 \\ 0 & 0 & -\frac{r_c}{L_c} \\ 0 & 0 & -2\pi \times 60 \\ -R_d\frac{k_{\mathrm{id}}^p + r_f}{L_f} + \frac{1}{C_f} & -(2\pi \times 60)R_d & R_d\frac{r_c}{L_c} - \frac{1}{C_f} \\ (2\pi \times 60)R_d & -R_d\frac{k_{\mathrm{id}}^p + r_f}{L_f} + \frac{1}{C_f} & 0 \end{bmatrix}$$
$$\begin{bmatrix} 0 & -\frac{1}{L_f} & 0 \\ 0 & 0 & -\frac{1}{L_f} \\ 2\pi \times 60 & \frac{1}{L_c} & 0 \\ -\frac{r_c}{L_c} & 0 & \frac{1}{L_c} \\ 0 & -R_d(\frac{1}{L_c} + \frac{1}{L_f}) & 2\pi \times 60 \\ R_d\frac{r_c}{L_c} - \frac{1}{C_f} & -2\pi \times 60 & -R_d(\frac{1}{L_c} + \frac{1}{L_f}) \end{bmatrix},$$

$$A_{LCL}^{\mathrm{CC}} = \begin{bmatrix} \frac{k_{\mathrm{id}}^i}{L_f} & 0 \\ 0 & \frac{k_{\mathrm{iq}}^i}{L_f} \end{bmatrix},$$

$$A_{LCL}^{\mathrm{PC}} = \begin{bmatrix} 0 & -\frac{k_{\mathrm{id}}^p}{L_f}k_Q^p & 0 & \frac{k_{\mathrm{id}}^p}{L_f}k_Q^i \\ -\frac{k_{\mathrm{iq}}^p}{L_f}k_P^p & 0 & \frac{k_{\mathrm{iq}}^p}{L_f}k_P^i & 0 \end{bmatrix},$$

$$A_{\mathrm{CC}}^{LCL} = \begin{bmatrix} -1 & 0 & 0 & 0 & 0 & 0 \\ 0 & -1 & 0 & 0 & 0 & 0 \end{bmatrix},$$

$$A_{\mathrm{CC}}^{\mathrm{PC}} = \begin{bmatrix} 0 & -k_Q^p & 0 & k_Q^i \\ -k_P^p & 0 & k_P^i & \end{bmatrix},$$

$$A_{\mathrm{PC}} = \begin{bmatrix} -\omega_c & 0 & 0 & 0 \\ 0 & -\omega_c & 0 & 0 \\ -1 & 0 & 0 & 0 \\ 0 & -1 & 0 & 0 \end{bmatrix}, A_{\mathrm{PLL}} = \begin{bmatrix} -\omega_{c,\mathrm{PLL}} & 0 & 0 \\ -1 & 0 & 0 \\ -k_{\mathrm{PLL}}^p & k_{\mathrm{PLL}}^i & 0 \end{bmatrix},$$

$$B_{LCL} = \begin{bmatrix} 0 & \frac{k_{\mathrm{id}}^p}{L_f}k_Q^p \\ \frac{k_{\mathrm{iq}}^p}{L_f}k_P^p & 0 \\ 0 & 0 \\ 0 & 0 \\ 0 & \frac{k_{\mathrm{id}}^p}{L_f}k_Q^p R_d \\ \frac{k_{\mathrm{iq}}^p}{L_f}k_P^p R_d & 0 \end{bmatrix}, B_{\mathrm{CC}} = \begin{bmatrix} 0 & k_Q^p \\ k_P^p & 0 \end{bmatrix},$$

$$B_{\mathrm{PC}} = \begin{bmatrix} 0 & 0 \\ 0 & 0 \\ 1 & 0 \\ 0 & 1 \end{bmatrix}.$$

The nonzero entries of $\widehat{g}(\widehat{\underline{x}}, \underline{u}_2)$ are given by

$$\widehat{g}_3(\widehat{\underline{x}}, \underline{u}_2) = (-k_{\mathrm{PLL}}^p v_{\mathrm{PLL}} + k_{\mathrm{PLL}}^i \phi_{\mathrm{PLL}})i_o^{\mathrm{q}} - \frac{\kappa}{L_c}v_g^{\mathrm{d}}(\widehat{\underline{x}}, \underline{u}_2),$$
$$\widehat{g}_4(\widehat{\underline{x}}, \underline{u}_2) = (k_{\mathrm{PLL}}^p v_{\mathrm{PLL}} - k_{\mathrm{PLL}}^i \phi_{\mathrm{PLL}})i_o^{\mathrm{d}} - \frac{\kappa}{L_c}v_g^{\mathrm{q}}(\widehat{\underline{x}}, \underline{u}_2),$$
$$\widehat{g}_5(\widehat{\underline{x}}, \underline{u}_2) = (-k_{\mathrm{PLL}}^p v_{\mathrm{PLL}} + k_{\mathrm{PLL}}^i \phi_{\mathrm{PLL}})(-R_d i_l^{\mathrm{q}} + v_o^{\mathrm{q}}) + \frac{R_d}{L_c}v_g^{\mathrm{d}}(\widehat{\underline{x}}, \underline{u}_2),$$
$$\widehat{g}_6(\widehat{\underline{x}}, \underline{u}_2) = (k_{\mathrm{PLL}}^p v_{\mathrm{PLL}} - k_{\mathrm{PLL}}^i \phi_{\mathrm{PLL}})(-R_d i_l^{\mathrm{d}} + v_o^{\mathrm{d}})$$

$$+\frac{R_d}{L_c}v_g^{\mathrm{q}}(\widehat{\underline{x}},\underline{u}_2),$$

$$\widehat{g}_9(\widehat{\underline{x}},\underline{u}_2)=\frac{3}{2}\omega_c\left(v_g^{\mathrm{d}}(\widehat{\underline{x}},\underline{u}_2)i_o^{\mathrm{d}}+v_g^{\mathrm{q}}(\widehat{\underline{x}},\underline{u}_2)i_o^{\mathrm{q}}\right),$$

$$\widehat{g}_{10}(\widehat{\underline{x}},\underline{u}_2)=\frac{3}{2}\omega_c\left(v_g^{\mathrm{q}}(\widehat{\underline{x}},\underline{u}_2)i_o^{\mathrm{d}}-v_g^{\mathrm{d}}(\widehat{\underline{x}},\underline{u}_2)i_o^{\mathrm{q}}\right),$$

$$\widehat{g}_{13}(\widehat{\underline{x}},\underline{u}_2)=\omega_{c,\mathrm{PLL}}v_g^{\mathrm{d}}(\widehat{\underline{x}},\underline{u}_2),$$

$$\widehat{g}_{15}(\widehat{\underline{x}},\underline{u}_2)=2\pi\times 60,$$

where $v_g^{\mathrm{d}}(\widehat{\underline{x}},\underline{u}_2)$ and $v_g^{\mathrm{q}}(\widehat{\underline{x}},\underline{u}_2)$ are given by

$$v_g^{\mathrm{d}}(\widehat{\underline{x}},\underline{u}_2)=\frac{2}{3}\left(\cos(\delta)v_g^{\mathrm{a}}+\cos(\delta-\frac{2\pi}{3})v_g^{\mathrm{b}}+\cos(\delta+\frac{2\pi}{3})v_g^{\mathrm{c}}\right),$$

$$v_g^{\mathrm{q}}(\widehat{\underline{x}},\underline{u}_2)=\frac{2}{3}\left(\sin(\delta)v_g^{\mathrm{a}}+\sin(\delta-\frac{2\pi}{3})v_g^{\mathrm{b}}+\sin(\delta+\frac{2\pi}{3})v_g^{\mathrm{c}}\right).$$

REFERENCES

[1] "800,000 Microinverters Remotely Retrofitted on Oahu in One Day." http://spectrum.ieee.org/energywise/green-tech/solar/in-one-day-800000-microinverters-remotely-retrofitted-on-oahu. Accessed: 2017-03-14.

[2] "Our Plans for the Future." https://www.hawaiianelectric.com/about-us/our-vision/100-percent-renewable-energy. Accessed: 2017-03-14.

[3] C. T. Pan and Y. H. Liao, "Modeling and control of circulating currents for parallel three-phase boost rectifiers with different load sharing," *IEEE Transactions on Industrial Electronics*, vol. 55, pp. 2776–2785, July 2008.

[4] T. P. Chen, "Dual-modulator compensation technique for parallel inverters using space-vector modulation," *IEEE Transactions on Industrial Electronics*, vol. 56, pp. 3004–3012, August 2009.

[5] D. Wu, Z. Guo, D. Sha, Z. Qin, and X. Liao, "Parallel-connected three-phase inverters for railway auxiliary power supply without sensing output currents," in *IEEE Applied Power Electronics Conference and Exposition*, pp. 136–140, February 2012.

[6] J. A. Mueller, M. Rasheduzzaman, and J. W. Kimball, "A model modification process for grid-connected inverters used in islanded microgrids," *IEEE Transactions on Energy Conversion*, vol. 31, pp. 240–250, March 2016.

[7] J. H. Chow, R. Galarza, P. Accari, and W. W. Price, "Inertial and slow coherency aggregation algorithms for power system dynamic model reduction," *IEEE Transactions on Power Systems*, vol. 10, pp. 680–685, May 1995.

[8] L. Luo and S. V. Dhople, "Spatiotemporal model reduction of inverter-based islanded microgrids," *IEEE Transactions on Energy Conversion*, vol. 29, pp. 823–832, December 2014.

[9] M. Rasheduzzaman, J. A. Mueller, and J. W. Kimball, "Reduced-order small-signal model of microgrid systems," *IEEE Transactions on Sustainable Energy*, vol. 6, pp. 1292–1305, October 2015.

[10] P. J. Hart, R. H. Lasseter, and T. M. Jahns, "Reduced-order harmonic modeling and analysis of droop-controlled distributed generation networks," in *IEEE 7th International Symposium on Power Electronics for Distributed Generation Systems (PEDG)*, pp. 1–9, June 2016.

[11] K. Kodra, N. Zhong, and Z. Gajić, "Model order reduction of an islanded microgrid using singular perturbations," in *American Control Conference (ACC)*, pp. 3650–3655, July 2016.

[12] M. Calabria and W. Schumacher, "Modeling power inverter interactions in a low voltage grid," in *IEEE 15th Workshop on Control and Modeling for Power Electronics (COMPEL)*, pp. 1–9, June 2014.

[13] A. Ulbig, T. S. Borsche, and G. Andersson, "Impact of low rotational inertia on power system stability and operation," 2014. [Online] Available at: `http://arxiv.org/abs/1312.6435`.

[14] F. Katiraei, M. R. Iravani, and P. W. Lehn, "Small-signal dynamic model of a micro-grid including conventional and electronically interfaced distributed resources," *IET Generation, Transmission Distribution*, vol. 1, pp. 369–378, May 2007.

[15] "Sinvert pvs 600series central inverters and components for photovoltaic power plants." http://www.renelux.com/Acrobat/Products/Inverters/SIEMENS/SINVERT_PVS_Brochure_English_2012-04.pdf. Accessed: 2016-12-20.